Inorganic Chemistry

Article

pubs.acs.org/IC

Comparison of the Effect of Functional Groups on Gas-Uptake Capacities by Fixing the Volumes of Cages A and B and Modifying the Inner Wall of Cage C in rht-Type MOFs

XiaoLiang Zhao,[†] Di Sun,[†] Shuai Yuan,[†] Shengyu Feng,[†] Rong Cao,[‡] Daqiang Yuan,*[,‡] Suna Wang,[§] Jianmin Dou,[§] and Daofeng Sun*[,†]

[†]Key Lab for Colloid and Interface Chemistry of Education Ministry, School of Chemistry and Chemical Engineering, Shandong University, Jinan 250100, People's Republic of China

[‡]State Key Laboratory of Structural Chemistry, Fujian Institute of Research on the Structure of Matter, Chinese Academy of Sciences, Fujian, Fuzhou 350002, People's Republic of China

[§]Shandong Provincial Key Laboratory of Chemical Energy Storage and Novel Cell Technology, School of Chemistry and Chemical Engineering, Liaocheng University, Liaocheng 252059, China

Supporting Information

ABSTRACT: Three porous (3,24)-connected rht-type metal−organic frameworks (MOFs), $[Cu_3L(H_2O)_3]\cdot$xsolvents (H_6L^{OH} = 4,4′,4″-(hydroxysilanetriyl)tris-(triphenyl-3,5-dicarboxylic acid), **SDU−6**; H_6L^{Me} = 4,4′,4″-(methylsilanetriyl)tris-(triphenyl-3,5-dicarboxylic acid), **SDU−7**; H_6L^{iBu} = 4,4′,4″-(isobutylsilanetriyl)tris-(triphenyl-3,5-dicarboxylic acid), **SDU−8**), have been successfully prepared from $[Cu_2(COO)_4]$ paddlewheel SBUs (secondary building units) and C_3-symmetric Si-based hexatopic carboxylatelinkers. All porous MOFs are constructed from 3D packing of nanosized cuboctahedral, truncated tetrahedral, and truncated octahedral cages. **SDU−6−8** differ only in the functionality of the central Si atom of the hexacarboxylate ligands with hydroxyl, methyl, and isobutyl groups, respectively. Gas adsorption measurements of activated MOFs suggested that decoration of the cage walls with strong polar groups can enhance the adsorption capacities for N_2, H_2, and CH_4. **SDU−6** with −OH as the functional group possesses high CH_4 uptake (172 $cm^3\ cm^{-3}$ at 35 bar), which is very close to DOE target of 180 $cm^3\ cm^{-3}$.

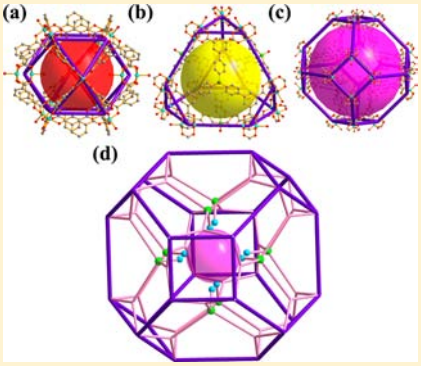

INTRODUCTION

Metal−organic frameworks (MOFs) built from metal-based nodes and organic polycarboxylate linkers are of enormous interest as a novel class of microporous material due to their important applications in a wide range of fields including gas storage/separation, catalysis, nonlinear optics, electronics, and drug delivery.[1−6] So far, construction of MOFs with high gas-uptake capacity remains a great challenge. On the basis of current research on how to improve the gas-uptake for a desired MOF, two efficient strategies can be achieved: one is to predesign the organic ligand by decorating it with a functional organic group that has high binding affinity to gas molecules;[7] the other one is the postsynthesis modification of the organic ligand after the framework was formed.[8] The latter strategy requires the porous frameworks possessing high stability that can sustain the organic reaction on the ligands under certain condition. Since most of the porous MOFs are sensitive to acid and base and cannot keep their frameworks during the postsynthesis modification, hence, the former one becomes a promising strategy on design and synthesis of porous materials with improved gas adsorption capacity. Recently, a large number of porous MOFs with enhanced gas uptake have been designed and synthesized through predesigning the organic ligand. Notable examples include (3,24)-connected nets or rht-type MOFs based on copper paddlewheel $[Cu_2(COO)_4]$ building blocks and C_3-symmetric hexacarboxylate linkers.[7,9] This family of porous materials possesses highly attractive because they normally have high surface area and can be easily constructed from C_3-symmetric hexacarboxylate linkers. Such MOFs were first reported by Eddaoudi and co-workers in CuTZI (H_3TZI = 5-tetrazolylisophthalic acid) based on supermolecular building blocks.[10] Thereafter, some remarkable results were reported by several other research groups. In particular, Zhou reported an isoreticular PCN-6X series generated from a series of hexacarboxylate ligands incorporating rigid C≡C triple bonds.[9i−k] The *de novo* synthesis of NU-100 with ultrahigh surface area and gas storage capacities was also documented by Hupp and co-workers.[9b] In this family of porous materials, there contain three types of cages (Figure 1): a cuboctahedron (Cage A), a truncated tetrahedron (Cage B), and a truncated octahedron (Cage C). Cage A is made up of 24 Cu^{II} ions (12 paddlewheel SBUs) and 24 isophthalate moieties, hence, the volume of Cage A is fixed and would not be changed

Received: July 12, 2012
Published: September 18, 2012

   dx.doi.org/10.1021/ic3015207 | *Inorg. Chem.* 2012, 51, 10350−10355

Figure 1. Schematic representation of the cuboctahedron (Cage A, left), truncated tetrahedron (Cage B, middle), and truncated octahedron (Cage C, right) existing in rht-type MOFs based on copper paddlewheel $[Cu_2(COO)_4]$ building blocks and C_3-symmetric hexacarboxylate linkers.

no matter what size of organic ligands is used. However, the volumes of Cages B and C are adjustable if different sizes of organic ligands are used in the assembly of the porous materials. Thus, the gas adsorption capacity of this family of materials can be tuned by functionalizing the central core of the hexacarboxylate ligands or enlarging the volumes of Cages B and C. Very recently, Bai and co-workers reported a rht-type MOF with enhanced CO_2 binding affinity by decorating the central core of the hexacarboxylate ligand with anacylamide-group.[7b] Schröder and co-workers compared the effect of the functionality of the central core of the hexacarboxylate ligands on the gas adsorption capacity.[9h] Although the volume of Cage A is fixed in their work, the organic ligands used differ in the size, resulting in the different volumes of Cages B and C.

In this contribution, we mainly focus our attention on the study of the effect of functional central core of the hexacarboxylate ligands (Figure 2) on the gas adsorption

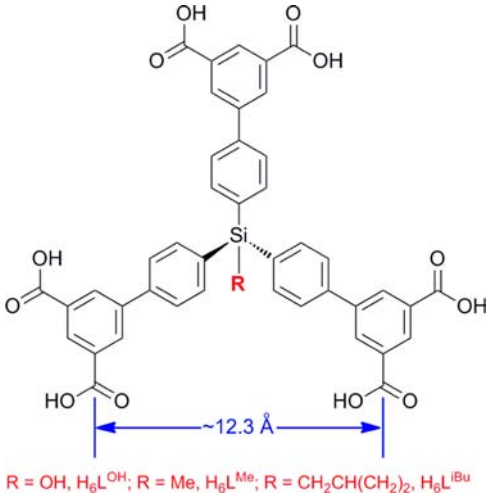

Figure 2. The chemical structure of H_6L ligands.

capacity by fixing the volumes of Cages A and B and modifying the inner wall of Cage C. Our work is illustrated with the design and synthesis of three isostructural rht-type MOFs, Cu_3L [H_6L^{OH} = 4,4′,4″- (hydroxysilanetriyl)tris(triphenyl-3,5-dicarboxylic acid), **SDU−6**; H_6L^{Me} = 4,4′,4″-(methylsilanetriyl)tris-(triphenyl-3,5-dicarboxylic acid), **SDU−7**; H_6L^{ibu} = 4,4′,4″-(isobutylsilanetriyl)tris(triphenyl- 3,5-dicarboxylic acid), **SDU−8**; **SDU** stands for Shandong University], based on three well-designed organic ligands decorated with −OH, $-CH_3$, and $-CH_2CH(CH_3)_2$ on the central core of the hexacarboxylate ligands, respectively, which possess the same length. The effect of the functional groups [−OH, $-CH_3$, $-CH_2CH(CH_3)_2$] on the adsorption capacities of N_2, H_2, and CH_4 has been fully studied.

RESULTS AND DISCUSSION

Synthesis. In the past decade, a series of porous MOFs based on trigonal hexatopic carboxylate ligands and paddle-wheel SBUs have been designed and synthesized. All these porous materials possess (3, 24)-connected nets or rht-type topologies. As far as is known, most of the organic ligands used to construct rht-type MOFs have C_3 symmetry in which the three isophthalate units are almost coplanar. We are particularly interested in the construction of highly porous materials based on C_3-symmetric hexacarboxylate ligands with three isophthalate units being noncoplanar. Very recently, we reported a (4,8)-connected flu-type network based on a tetrapodal silicon-based linker.[11] In this contribution, continuing our previous work on organosiliconcarboxylate ligands, we designed and synthesized a new type of tapered hexacarboxylate ligands through modifying the tetrahedral silicon center by replacing one of its four benzoic acid moieties with an arbitrary functional group, such as −OH, $-CH_3$, and $-CH_2CH(CH_3)_2$, and their solvothermal assembly with copper SBU resulted in the formation of three isostructural MOFs with the same rht-type network. The size of the three ligands is comparable to 5,5′,5″-benzene-1,3,5-triyltris(1-ethynyl- 2-isophthalate) in PCN-61.[9i,k]

Structural Description. **SDU−6−8** were characterized by single-crystal X-ray crystallography, powder X-ray diffraction (PXRD), thermogravimetric analysis (TGA), and elemental analysis. The PXRD confirmed the phase purities of the bulk samples (Figures S4−6). The dissimilarities intensity may be due to the preferred orientation of the crystalline powder samples. Moreover, the PXRD patterns of bulky crystalline samples after the adsorption experiments are also similar to those simulated patterns, which further supported the sustained porosity. TGA curves revealed that **SDU−6−8** loses all solvents before 304 °C (Figures S1−3).

Single-crystal X-ray structural studies confirmed that the frameworks of **SDU−6−8** are isostructural, and they differ only in the functional group of Si-based hexatopic carboxylate. All crystallize in the cubic space group $Fm\bar{3}m$ with large unit cells (~43 Å). **SDU−6−8** have the same (3, 24)-connected rht topology as reported structures. In all cases, each carboxyl group of the ligand bridges two Cu^{II} ions to form a dicopper paddlewheel $[Cu_2(COO)_4]$ SBU. Each ligand connects six $[Cu_2(COO)_4]$ SBUs to form a hexagonal face of the truncated tetrahedron and truncated octahedron (Figure 3a and 3b). The ligands can be considered as a 3-connected node, containing three noncoplanar isophthalate units. Different from other coplanar rigid hexatopic carboxylates, the Si-based hexatopic carboxylates adopt a tripod-like geometry with Si atom deviating the plane defined by 12 O atoms of 3.44, 3.54, and 3.70 Å for L^{OH}, L^{Me}, and L^{iBu}, respectively, which can create the curvature of pores or nonlinearity of channels and effectively enlarge the interior surface area, potentially enhancing the gas uptake abilities.

All frameworks have the similar sized cuboctahedral cage (Figure 3c), constructed from 24 isophthalate fragments and 12 $[Cu_2(COO)_4]$ paddlewheels, which serves as a 24-connected node. Thus, the isostructural frameworks in **SDU−6−8** form (3, 24)-connected networks. The frameworks can also be viewed in terms of nanosized cages packed through sharing faces with three types of cages, Cage A, Cage B, and Cage C, in a 1:2:1 ratio (Figure 3d). In details, each Cage B is connected

dx.doi.org/10.1021/ic3015207 | Inorg. Chem. 2012, 51, 10350−10355

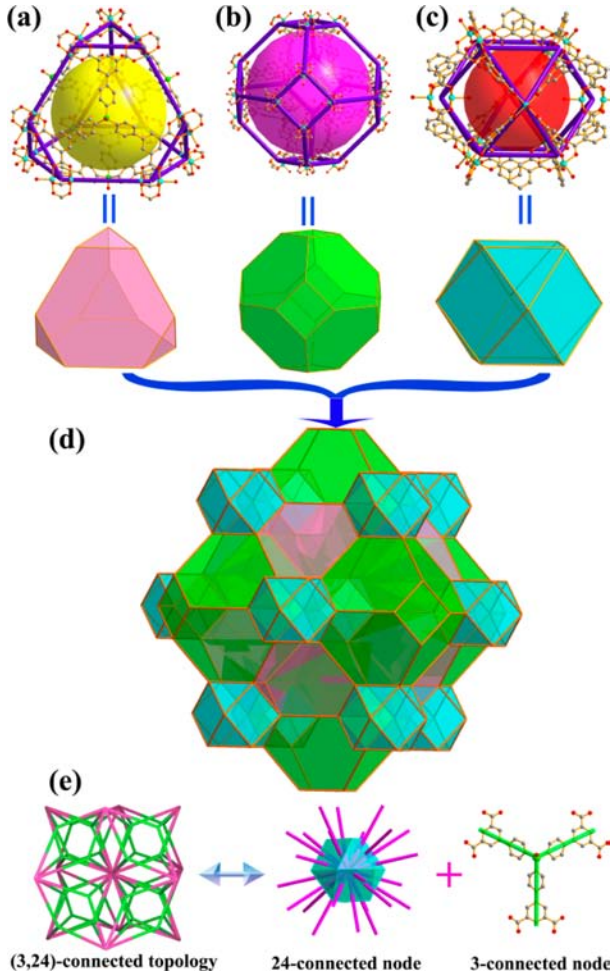

Figure 3. Structural features of **SDU−6**: (a) truncated tetrahedral cage, (b) truncated octahedral cage, (c) cuboctahedral cage (Cu: cyan; Si: green; C: gray; O: red), (d) 3D packing of three types of polyhedra in **SDU−6**, and (e) (3,24)-connected rht topology.

to four Cage A by sharing of triangular windows, and each Cage A is surrounded by eight Cage C, and each Cage C is connected to six Cage A by sharing the truncated vertices which are the square windows formed by the $[Cu_2(COO)_4]$ paddlewheels. Different from other reports that the sizes of Cages B and C are distinct when different organic ligands are used, Cages A and B are fixed in **SDU−6−8**, with the approximate cavity radius of 6.6 and 6.7 Å, respectively (Table 1). The functional groups such as $-OH$, $-CH_3$, $-CH_2CH(CH_3)_2$ in **SDU−6−8** hange on the inner wall of Cage C and point toward the center of the cage (Figure 4). It is clear that the cavity size of Cage C decreases with the increase of the size of the inner functional

Table 1. Cage Sizes, Surface Areas, Pore Volumes, and Porosities of SDU−6−8

	SDU−6	SDU−7	SDU−8
Cage A (Å)[a]	6.57	6.57	6.62
Cage B (Å)[a]	6.67	6.73	6.61
Cage C (Å)[a]	5.96	5.61	4.47
porosity[a]	70.6%	70.3%	68.2%
pore volume ($cm^3\ g^{-1}$) calc.[a]/ exptl.	1.15/1.17	1.16/1.10	1.06/1.02
surface area ($m^2\ g^{-1}$) calc.[b]/ BET	2987/2826	2960/2713	2741/2516

[a]Calculated using Platon. [b]Calculated using poreblazer.

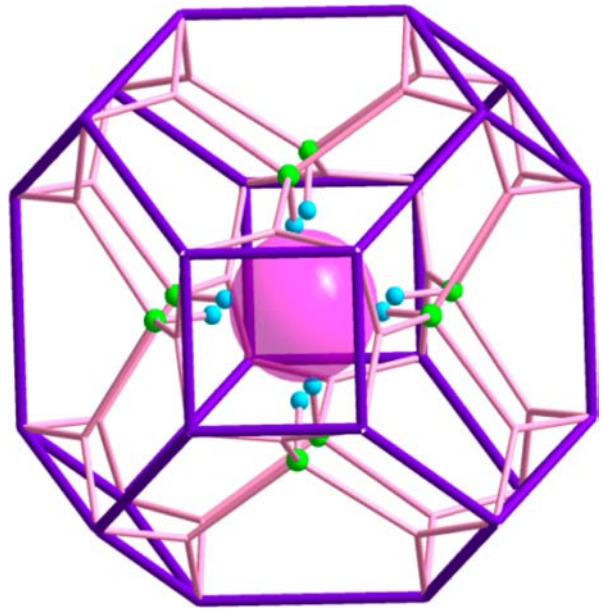

Figure 4. Highlighting Cage C showing all the functional groups on the center core of the ligands pointing toward the center of the cage. Green ball, Si atom; light blue ball, functional groups such as $-OH$, $-CH_3$, and $-CH_2CH(CH_3)_2$.

groups, which results in the changes of the cavity radius from 6.0, 5.6 to 4.5 Å in **SDU−6−8**, respectively. Thus, the only difference among **SDU−6−8** is the existence of different functional groups in Cage C, which provide us a great chance to systematically compare the effect of the functional groups on the gas adsorption capacity and pore structure (see below). The total solvent-accessible volumes for the desolvated frameworks after removal of guest solvents and coordinated water molecules are estimated to be 70.6% (**SDU−6**), 70.3% (**SDU−7**), and 68.2% (**SDU−8**) calculated by the *PLATON/VOID* routine (probe radius = 1.80 Å).[12] The calculated pore volume of the desolvated frameworks are 1.15, 1.16, and 1.06 $cm^3\ g^{-1}$ for **SDU−6−8**, respectively (Table 1).

N_2 Adsorption of SDU−6−8. To check the permanent porosities of **SDU−6−8**, the freshly prepared samples were soaked in methanol and dichloromethane to exchange the less volatile DEF solvent, followed by evacuation under a dynamic vacuum at 80 °C overnight. A color change from bright-blue to purple-blue occurred, indicating that open Cu(II) sites have been generated similar to those observed for other frameworks.[13] As shown in Figure 5, desolvated **SDU−6−8** display typical Type-I adsorption isotherms, suggesting the retention of the microporous structures after the removal of solvents from the crystalline samples. All sets of isotherms show slight changes of slope between 0.01 to 0.1 bar, indicating that the different sized pores are filled in sequence as the pressure increases from below 0.01 to 0.1 bar. **SDU−6−8** adsorb 753, 713, and 659 $cm^3\ g^{-1}$ of N_2 at 77 K, respectively. These values are comparable to those of NOTT-102 (736 $cm^3\ g^{-1}$), NOTT-110 (768 $cm^3\ g^{-1}$), and NOTT-111 (790 $cm^3\ g^{-1}$).[14] The total pore volumes of 1.17, 1.10, and 1.02 $cm^3\ g^{-1}$ for **SDU−6−8**, respectively, were calculated from the N_2 isotherms (P/P_0 = 0.98), which are very close to the theoretical results (Table 1). Fitting the N_2 isotherms using the low-pressure region data

dx.doi.org/10.1021/ic3015207 | *Inorg. Chem.* 2012, 51, 10350−10355

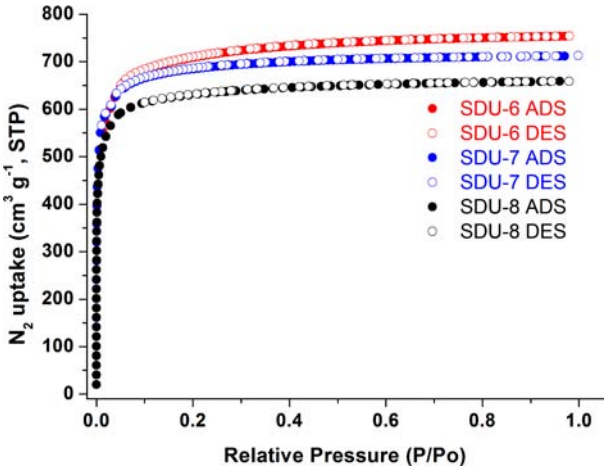

Figure 5. The N_2 sorption isotherms at 77 K for **SDU−6−8** (solid circles: adsorption; open circles: desorption).

afforded Brunauer−Emmett−Teller (BET) surface areas of 2826, 2713, and 2516 m^2 g^{-1} for **SDU−6−8**, respectively (Figures S7−9), which show a good agreement with the calculated data using the crystal data by poreblazer V1.2 (Table 1).[15] The maximum N_2 uptake decreases from 756 cm^3 g^{-1} for **SDU−6** to 659 cm^3 g^{-1} for **SDU−8** at 77 K, consistent with their respective surface areas and pore volumes. The BET surface areas of them are much smaller than the record for MOF-210 (6240 m^2 g^{-1}) and are comparable to NOTT-103 (2929 m^2 g^{-1}).[14a,16]

In order to have a preliminary understanding of the effect of functional group on pore structure, the pore size distribution data of **SDU−6−8** were calculated by nonlocal density functional theory (NLDFT) using N_2 isotherm data (Figure 6). The pore size distributions of **SDU−6−8** are very similar,

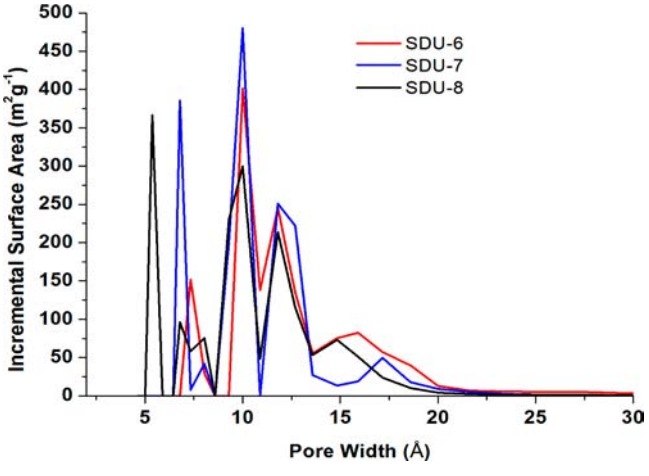

Figure 6. Pore size distribution of **SDU−6−8**.

and the major pore size distributes between 9 and 13 Å, which correspond with the crystal model. Due to the lack of suitable models for MOFs in NLDFT, the difference of pore size distribution among **SDU-6−8** is not distinct. Therefore, the theoretic pore size distributions were calculated using the Monte Carlo procedure (Figure S10),[17] in which the effect of the functional group is clear. The contribution of Cages A and B in **SDU−6−8** to pore size distribution are almost the same in the range of 12−14 Å, while the values for Cage C shift from 11.5, 10.9 to 8.3 Å. The results indicate that the bulky group in silicon can reduce the effective pore size of Cage C.

H_2 Adsorption of SDU−6−8. Low-pressure H_2 uptakes of desolvated samples of **SDU−6−8** were continuously determined using volumetric gas adsorption measurements. As demonstrated in Figure 7, the desolvated **SDU−6−8** exhibit

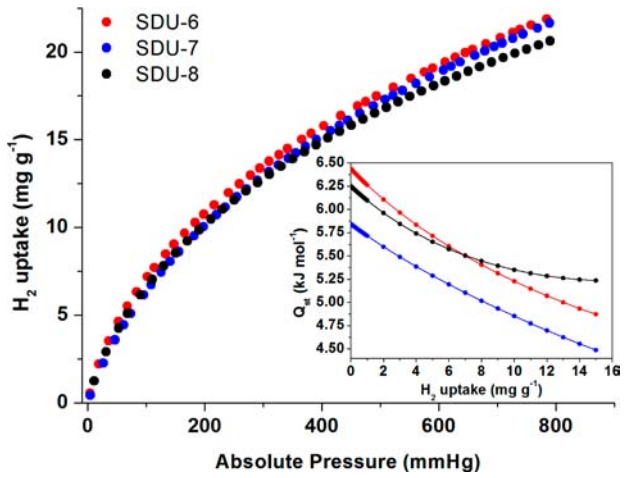

Figure 7. Low-pressure H_2 adsorption isotherms for **SDU−6−8** at 77 K. For clarity, the desorption data are not plotted. Insert shows the isosteric heat of adsorption for H_2 in **SDU−6−8**.

the classical reversible Type-I for H_2 adsorption isotherms expected for microporous materials. The adsorption isotherms exhibit 21.5, 21.3, and 20.3 mg g^{-1} H_2 uptake for **SDU−6−8**, respectively, under the conditions of 77 K and 1 bar, which are comparable or even superior to previously reported MOFs incorporating Cu(II) paddlewheel SBUs, such as PCN-61 (23.0 mg g^{-1} at 77 K, 1 bar) and NOTT-112 (23.5 mg g^{-1} at 77 K, 800 mmHg).[9d,i] The higher H_2 uptake capability of **SDU−6** compared to the other two is attributed to its larger surface areas as well as the stronger polar hydroxyl group, producing stronger dipole−induced dipole interaction between H_2 and the hydroxyl group. However, in the low-pressure region (<200 mmHg), the H_2 uptake of **SDU−8** is slightly larger than **SDU−7** (Figure S11), which shows that the isobutyl group increases the hydrogen affinity toward the framework compared with methyl group. It can be interpreted as the bulky functional group decreases the pore size and enhances the roughness of pore surface, which will be quantified by the H_2 isosteric heat of adsorption (Q_{st}). The Q_{st} of **SDU−6−8** were calculated by fitting the H_2 adsorption isotherms at 77 and 87 K to a Virial-type expression (Figures S12−14). The Q_{st} have the estimated value of 6.43, 5.84, and 6.25 kJ mol^{-1} for **SDU−6−8** (Figure 7), respectively, at the lowest coverage, which values can be compared with other (3, 24)-connected nets.[9] The trend is identical with the proposed analysis: the order of contribution to hydrogen affinity in **SDU−6−8** is polar hydroxyl group > isobutyl group > methyl group.

In the high pressure range, it can be found that the surface area dominates the maximum excess gravimetric H_2 uptake capacity in **SDU−6−8** (Figure 8). This correlation has also been observed in other isostructural MOFs series.[9i,14a] The excess H_2 uptakes reach up to the maximum at about 32 bar and 77 K for all three MOFs. Due to the highest surface area of **SDU−6**, it has the highest maximum excess H_2 uptake capacity (57.3 mg g^{-1}), which value is slightly lower than that of PCN-

dx.doi.org/10.1021/ic3015207 | Inorg. Chem. 2012, 51, 10350−10355

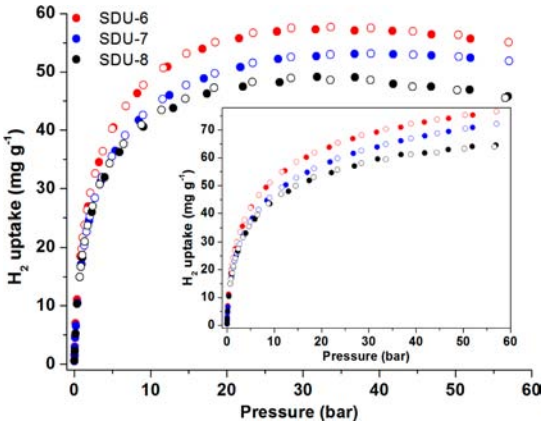

Figure 8. Excess H_2 adsorption isotherms for **SDU−6−8** at 77 K up to 60 bar. Insert shows total adsorption isotherm. (Solid symbols: adsorption; empty symbols: desorption).

61 (62.4 mg g^{-1}). Also, **SDU−6** and **−7** have the saturation hydrogen uptakes of 53.1 and 49.1 mg g^{-1}, respectively. Taking into consideration of the gaseous hydrogen compressed within the framework void, the total gravimetric and volumetric H_2 uptake of **SDU−6−8** will be 76.3, 71.6, and 64.5 mg g^{-1} and 46.6, 43.5, and 39.2 g L^{-1}, respectively, at 55 bar (Figure 8).

CH_4 Adsorption of SDU−6−8. As shown in Figure 9, at 298 K and 35 bar, the excess gravimetric CH_4 uptake capacity

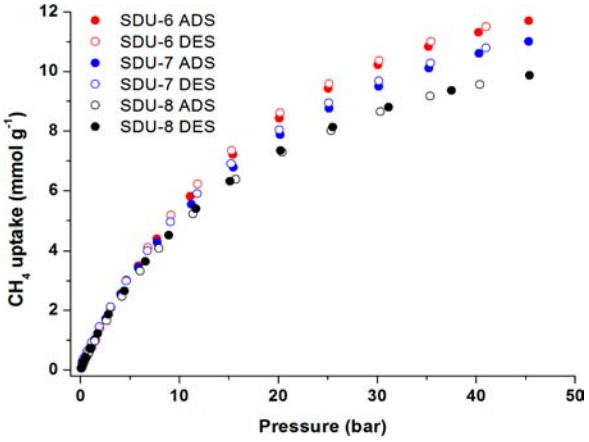

Figure 9. Excess CH_4 adsorption isotherms for **SDU−6−8** at 298 K up to 45 bar.

of **SDU−6−8** is 10.8, 10.1, and 9.1 mmol g^{-1}, which correspond to the volumetric values of 148, 137, and 125 cm^3 cm^{-3} based on the crystallographic density (Figure S15). The total volumetric CH_4 uptake capacity of **SDU−6** is as high as 172 cm^3 cm^{-3} at 35 bar (Figure S16), which is close to the DOE target of 180 cm^3 cm^{-3} and is among the highest methane uptakes of all the reported MOFs materials.[17] Like the H_2 uptake, in the case of **SDU−6−8**, the CH_4 uptake capacity is controlled mainly by the surface area and polar functional group.

CONCLUSION

In conclusion, we prepared three (3, 24)-connected MOFs using $[Cu_2(COO)_4]$ paddlewheel SBUs and C_3-symmetric Si-based hexatopic carboxylates decorated by strong polar hydroxyl and weak polar methyl and isobutyl groups, respectively. Results and conclusions of these investigations are summarized as follows: 1) by introducing different functional groups on the central Si atom, a series of tapered hexatopic carboxylates have been synthesized, and their assembly with rigid paddlewheel SBUs resulted in the formation of rht-type MOFs; 2) the effect of functional groups on the gas adsorption capacities has been systemically studied for the first time by fixing the sizes of Cages A and B and modifying the inner wall of Cage C in rht-type MOFs; 3) they show similar high H_2, N_2, and CH_4 adsorption capacities, which are dependent on not only the larger surface areas and pore volumes but also the polarity decorated on the organic linkers. Our research results presented here further indicate that the polarity of the functional groups has a significant effect on the gas adsorption of an MOF and provide the information on the design and synthesis of porous MOFs with high gas adsorption capacity.

EXPERIMENTAL SECTION

All chemicals and solvents used in the syntheses were of analytical grade and used without further purification. H_6L^{OH}, H_6L^{Me}, and H_6L^{iBu} were synthesized using the literature method (see the Supporting Information). ^1H NMR spectra was measured on a Bruker AVANCE-300 NMR spectrometer. The thermogravimetric analysis (TGA) was carried out between room temperature and 800 °C in a static N_2 with a heating rate of 10 °C/min (Figures S1−3). Intensity data of the **SDU−6** and **SDU−7** were collected on a Bruker Apex II CCD diffractometer equipped with a fine-focus sealed-tube X-ray source (Mo Kα radiation, graphite monochromated). Intensity data of the **SDU−8** were collected on an Agilent Xcalibur Eos Gemini diffractometer equipped with Enhance (Cu) X-ray Source (Cu−Kα, λ = 1.54178 Å). X-ray powder diffractions were measured on a Bruker AXS D8 Advance. The low-pressure N_2 and H_2 sorption isotherm measurements were performed on an ASAP 2020 M accelerated surface area and porosimetry analyzer. High-pressure H_2 and CH_4 sorption isotherm measurements were performed using a Hydrogen Storage Analyzer HTP1-V.

The intensity data of **SDU−6** and **SDU−7** were collected at 173 K on a Bruker Apex II area detector diffractometer (Mo−Kα, λ = 0.71073 Å). The intensity data of **SDU−8** were collected at 140 K on an Agilent Xcalibur Eos Gemini diffractometer with Enhance (Cu) X-ray Source (Cu−Kα, λ = 1.54178 Å). Absorption corrections were applied by using the multiscan method. Data were integrated and corrected for Lorentz, polarization, and absorption effects. Space group determinations were made based on systematic absences, E statistics, and successful refinement of the structure. Structures were solved by direct method and refined by full-matrix least-squares on F^2 using *SHELXTL*. Non-hydrogen atoms were refined with anisotropic displacement parameters during the final cycles. Organic hydrogen atoms were placed in calculated positions with isotropic displacement parameters set to 1.2 or 1.5 × U_{eq} of the attached atom. In the structure of **SDU−8**, the isobutyl group is severly disordered around the C_3 axis, and attempts to locate and refine the isobutyl group were unsuccessful. Therefore, the theoretical model of the isobutyl group was attached to an Si atom. There are large solvent accessible void volumes in the crystals of **SDU−6−8** which are occupied by disordered DEF and water molecules. No satisfactory disorder model could be achieved, and therefore the *PLATON/SQUEEZE* routine was used to remove these electron densities.

ASSOCIATED CONTENT

Supporting Information

Crystallographic data in CIF format, additional figures of gas adsorptions, powder X-ray diffractions (PXRD) patterns, and the thermogravimetric analysis for **SDU-6−8**. This material is available free of charge via the Internet at http://pubs.acs.org. CCDC Nos. 880865−880867 for **SDU−6−8**.

AUTHOR INFORMATION

Corresponding Author

*E-mail: dfsun@sdu.edu.cn (D.S.). Fax: +86-531-88364218. E-mail: ydq@fjirsm.ac.cn (D.Y.).

Notes

The authors declare no competing financial interest.

ACKNOWLEDGMENTS

This work was supported by the NSFC (Grant Nos. 90922014, 20701025, 20801025), the Shandong Natural Science Fund for Distinguished Young Scholars (2010JQE27021), NSF of Fujian Province (2012J01058), Independent Innovation Foundation of Shandong University (2010JQ011 and 2011GN030) and the "One Hundred Talent Project" from Chinese Academy of Sciences.

REFERENCES

(1) (a) Zhou, H. C.; Long, J. R.; Yaghi, O. M. *Chem. Rev.* **2012**, *112*, 673. (b) Long, J. R.; Yaghi, O. M. *Chem. Soc. Rev.* **2009**, *38*, 1213. (c) Tanabe, K. K.; Cohen, S. M. *Chem. Soc. Rev.* **2011**, *40*, 498. (d) Ma, L.; Abney, C.; Lin, W. *Chem. Soc. Rev.* **2009**, *38*, 1248. (e) Yoon, M.; Srirambalaji, R.; Kim, K. *Chem. Rev.* **2012**, *112*, 1196. (f) Cui, Y. J.; Yue, Y. F.; Qian, G. D.; Chen, B. L. *Chem. Rev.* **2012**, *112*, 1126.

(2) (a) Rowsell, J. L.; Spencer, E. C.; Eckert, J.; Howard, J. A.; Yaghi, O. M. *Science* **2005**, *309*, 1350. (b) Makiura, R.; Motoyama, S.; Umemura, Y.; Yamanaka, H.; Sakata, O.; Kitagawa, H. *Nat. Mater.* **2010**, *9*, 565. (c) Bloch, E. D.; Queen, W. L.; Krishna, R.; Zadrozny, J. M.; Brown, C. M.; Long, J. R. *Science* **2012**, *335*, 1606. (d) Lu, G.; Li, S.; Guo, Z.; Farha, O. K.; Hauser, B. G.; Qi, X.; Wang, Y.; Wang, X.; Han, S.; Liu, X.; DuChene, J. S.; Zhang, H.; Zhang, Q.; Chen, X.; Ma, J.; Loo, S. C.; Wei, W. D.; Yang, Y.; Hupp, J. T.; Huo, F. *Nat. Chem.* **2012**, *4*, 310. (e) Matsuda, R.; Kitaura, R.; Kitagawa, S.; Kubota, Y.; Belosludov, R. V.; Kobayashi, T. C.; Sakamoto, H.; Chiba, T.; Takata, M.; Kawazoe, Y.; Mita, Y. *Nature* **2005**, *436*, 238.

(3) (a) Horike, S.; Inubushi, Y.; Hori, T.; Fukushima, T.; Kitagawa, S. *Chem. Sci.* **2012**, *3*, 116. (b) Mohideen, M. I.; Xiao, B.; Wheatley, P. S.; McKinlay, A. C.; Li, Y.; Slawin, A. M.; Aldous, D. W.; Cessford, N. F.; Duren, T.; Zhao, X.; Gill, R.; Thomas, K. M.; Griffin, J. M.; Ashbrook, S. E.; Morris, R. E. *Nat. Chem.* **2011**, *3*, 304. (c) McDonald, T. M.; Lee, W. R.; Mason, J. A.; Wiers, B. M.; Hong, C. S.; Long, J. R. *J. Am. Chem. Soc.* **2012**, *134*, 7056.

(4) (a) Li, H.; Eddaoudi, M.; O'Keeffe, M.; Yaghi, O. M. *Nature* **1999**, *402*, 276. (b) Kaye, S. S.; Dailly, A.; Yaghi, O. M.; Long, J. R. *J. Am. Chem. Soc.* **2007**, *129*, 14176.

(5) (a) Rowsell, J. L.; Yaghi, O. M. *Angew. Chem., Int. Ed.* **2005**, *44*, 4670. (b) Zhao, D.; Yuan, D. Q.; Zhou, H. C. *Energy Environ. Sci.* **2008**, *1*, 222. (c) Murray, L. J.; Dincă, M.; Long, J. R. *Chem. Soc. Rev.* **2009**, *38*, 1294. (d) Sculley, J.; Yuan, D.; Zhou, H.-C. *Energy Environ. Sci.* **2011**, *4*, 2721. (e) Suh, M. P.; Park, H. J.; Prasad, T. K.; Lim, D.-W. *Chem. Rev.* **2012**, *112*, 782.

(6) (a) Lin, X.; Jia, J.; Zhao, X.; Thomas, K. M.; Blake, A. J.; Walker, G. S.; Champness, N. R.; Hubberstey, P.; Schroder, M. *Angew. Chem., Int. Ed.* **2006**, *45*, 7358. (b) Banerjee, R.; Furukawa, H.; Britt, D.; Knobler, C.; O'Keeffe, M.; Yaghi, O. M. *J. Am. Chem. Soc.* **2009**, *131*, 3875. (c) O'Keeffe, M.; Yaghi, O. M. *Chem. Rev.* **2012**, *112*, 675.

(7) (a) Li, B.; Zhang, Z.; Li, Y.; Yao, K.; Zhu, Y.; Deng, Z.; Yang, F.; Zhou, X.; Li, G.; Wu, H.; Nijem, N.; Chabal, Y. J.; Lai, Z.; Han, Y.; Shi, Z.; Feng, S.; Li, J. *Angew. Chem., Int. Ed.* **2012**, *51*, 1412. (b) Zheng, B.; Bai, J.; Duan, J.; Wojtas, L.; Zaworotko, M. J. *J. Am. Chem. Soc.* **2011**, *133*, 748.

(8) (a) Cohen, S. M. *Chem. Rev.* **2012**, *112*, 970. (b) Morris, W.; Doonan, C. J.; Yaghi, O. M. *Inorg. Chem.* **2011**, *50*, 6853.

(9) (a) Luebke, R.; Eubank, J. F.; Cairns, A. J.; Belmabkhout, Y.; Wojtas, L.; Eddaoudi, M. *Chem. Commun.* **2012**, *48*, 1455. (b) Farha, O. K.; Özgür Yazaydın, A.; Eryazici, I.; Malliakas, C. D.; Hauser, B. G.; Kanatzidis, M. G.; Nguyen, S. T.; Snurr, R. Q.; Hupp, J. T. *Nat. Chem.* **2010**, *2*, 944. (c) Hong, S.; Oh, M.; Park, M.; Yoon, J. W.; Chang, J. S.; Lah, M. S. *Chem. Commun.* **2009**, 5397. (d) Yan, Y.; Lin, X.; Yang, S.; Blake, A. J.; Dailly, A.; Champness, N. R.; Hubberstey, P.; Schroder, M. *Chem. Commun.* **2009**, 1025. (e) Yan, Y.; Telepeni, I.; Yang, S. H.; Lin, X.; Kockelmann, W.; Dailly, A.; Blake, A. J.; Lewis, W.; Walker, G. S.; Allan, D. R.; Barnett, S. A.; Champness, N. R.; Schroder, M. *J. Am. Chem. Soc.* **2010**, *132*, 4092. (f) Yan, Y.; Yang, S.; Blake, A. J.; Lewis, W.; Poirier, E.; Barnett, S. A.; Champness, N. R.; Schroder, M. *Chem. Commun.* **2011**, *47*, 9995. (g) Zou, Y.; Park, M.; Hong, S.; Lah, M. S. *Chem. Commun.* **2008**, 2340. (h) Yan, Y.; Blake, A. J.; Lewis, W.; Barnett, S. A.; Dailly, A.; Champness, N. R.; Schroder, M. *Chem.—Eur. J.* **2011**, *17*, 11162. (i) Yuan, D. Q.; Zhao, D.; Sun, D. F.; Zhou, H. C. *Angew. Chem., Int. Ed.* **2010**, *49*, 5357. (j) Yuan, D.; Zhao, D.; Zhou, H. C. *Inorg. Chem.* **2011**, *50*, 10528. (k) Zhao, D.; Yuan, D. Q.; Sun, D. F.; Zhou, H. C. *J. Am. Chem. Soc.* **2009**, *131*, 9186.

(10) Nouar, F.; Eubank, J. F.; Bousquet, T.; Wojtas, L.; Zaworotko, M. J.; Eddaoudi, M. *J. Am. Chem. Soc.* **2008**, *130*, 1833.

(11) Zhao, X.; Zhang, L.; Ma, H.; Sun, D.; Wang, D.; Feng, S.; Sun, D. *RSC Adv.* **2012**, *2*, 5543.

(12) Spek, A. L. *J. Appl. Crystallogr.* **2003**, *36*, 7.

(13) Sun, D.; Ma, S.; Ke, Y.; Collins, D. J.; Zhou, H. C. *J. Am. Chem. Soc.* **2006**, *128*, 3896.

(14) (a) Lin, X.; Telepeni, I.; Blake, A. J.; Dailly, A.; Brown, C. M.; Simmons, J. M.; Zoppi, M.; Walker, G. S.; Thomas, K. M.; Mays, T. J.; Hubberstey, P.; Champness, N. R.; Schröder, M. *J. Am. Chem. Soc.* **2009**, *131*, 2159. (b) Yang, S.; Lin, X.; Dailly, A.; Blake, A. J.; Hubberstey, P.; Champness, N. R.; Schröder, M. *Chem.—Eur. J.* **2009**, *15*, 4829.

(15) Sarkisov, L.; Harrison, A. *Mol. Simulat.* **2011**, *37*, 1248.

(16) Furukawa, H.; Ko, N.; Go, Y. B.; Aratani, N.; Choi, S. B.; Choi, E.; Yazaydin, A. O.; Snurr, R. Q.; O'Keeffe, M.; Kim, J.; Yaghi, O. M. *Science* **2010**, *329*, 424.

(17) (a) Ma, S.; Sun, D.; Simmons, J. M.; Collier, C. D.; Yuan, D.; Zhou, H. C. *J. Am. Chem. Soc.* **2008**, *130*, 1012. (b) Guo, Z. Y.; Wu, H.; Srinivas, G.; Zhou, Y. M.; Xiang, S. C.; Chen, Z. X.; Yang, Y. T.; Zhou, W.; O'Keeffe, M.; Chen, B. L. *Angew. Chem., Int. Ed.* **2011**, *50*, 3178. (c) Wu, H.; Zhou, W.; Yildirim, T. *J. Am. Chem. Soc.* **2009**, *131*, 4995.